EXTERNALLY CORRECTED COUPLED-CLUSTER APPROACHES: ENERGY *versus* AMPLITUDE CORRECTED CCSD

Josef PALDUS[1,*] and Xiangzhu LI[2]

Department of Applied Mathematics, University of Waterloo, Waterloo, Ontario, Canada N2L 3G1; e-mail: [1] paldus@theochem.uwaterloo.ca, [2] xli@quantum.uwaterloo.ca

Received August 6, 2002
Accepted November 1, 2002

Laudatio

It is indeed a great pleasure to celebrate the 60th birthday of a trio of Czech and Slovak quantum chemists, Professors Petr Čársky, Ivan Hubač, and Miro Urban and to congratulate them on their many achievements, as well as to tell them how much their scientific contributions are appreciated and their personal friendship is valued. It has been a true delight for the senior co-author of this paper to take part in the Ph.D. Thesis supervision for two of them, and to watch their development during the intervening years. We all certainly look forward to their continued involvement in our scientific endeavours, since – to quote M. Émile Picard[1] – " ...l'âge de la retraite pour le professeur ne sera pas l'âge de la retraite pour le savant." In the future, we trust to see many important papers signed with their names and those of their students, and we wish them all only the best in their personal and professional lives.

The externally corrected coupled-cluster methods with singles and doubles (ecCCSD), which exploit some independently available wave function as a source of higher-than-pair clusters, are considered. The focus is on methods that employ a modest-size multireference (MR) configuration interaction (with singles and doubles, CISD) wave function as the external source. Both the amplitude- and energy-corrected CCSD methods are employed, the former correcting the standard single reference (SR) CCSD equations for triples and quadruples, while the latter accounts for the nondynamic correlation effects when evaluating the energy by employing the MR CISD wave function in lieu of the single determinantal (usually Hartree–Fock) reference in the asymmetric energy formula. The performance and relationship of both types of approaches is illustrated by computing the rotational and vibrational energy levels using the potential generated by these various methods and by comparing the calculated spectra with the experimental ones for the simplest first-row hydride, namely the LiH molecule. A special attention is paid to the role of core-correlation effects, in which case we also consider the HF molecule.

Keywords: Coupled-cluster methods; Multireference configuration interaction; Ro-vibrational spectra; LiH; HF; *Ab initio* calculations.

During the late sixties it became abundantly evident that the Hartree–Fock (HF) approximation[2–4], in spite of its conceptual importance and practical

usefulness, is unable to supply reliable and accurate information concerning many aspects of the molecular electronic structure. In particular, the so-called restricted HF (RHF) potential energy surfaces or curves invariably tend towards a wrong dissociation limit when breaking true chemical bonds, and the corresponding RHF dissociation energy may even become negative, as first realized in the well-known case of the F_2 molecule[5]. The situation becomes even more serious when considering certain nonenergetic properties (*cf.*, *e.g.*, refs[6,7]).

As with any independent particle model (IPM), the inadequacy of the HF approximation stems from its inability to properly account for the singular nature of the Coulomb potential, and thus to properly describe the many-electron correlation effects. Consequently, all present-day nonempirical quantitative studies of the molecular electronic structure exploit various post-HF methods. These are basically of two types, namely variational or perturbative.

Here we hasten to say that all *ab initio* approaches to the molecular electronic structure are based on model Hamiltonians. Even when we rely on the Born–Oppenheimer approximation and ignore all relativistic effects, the problem is unmanageable at the exact level once more than two electrons are involved, so that all molecular applications are based on models that are defined on finite-dimensional subspaces of a proper N-electron Hilbert space. In *ab initio* approaches, these subspaces – and the corresponding model Hamiltonians – are implied by the choice of the atomic orbital (AO) basis set, spanning the one-electron space, which in turn defines the N-electron space employed. The quality of the results obtained crucially depends on both the adequacy (essentially the size) of the AO basis set and the post-HF method employed. Needless to say that most post-HF approaches use the HF wave function as a reference.

The *variational* post-HF approaches are represented by various configuration interaction (CI) methods that exploit the Ritz variation principle and the linear Ansatz for the wave function in terms of the IPM states (or configurations). Unfortunately, the size of the CI problem, given by the dimension of the N-electron space employed, grows rapidly with the size of the system and the dimension of the one-electron space used, so that it is imperative to use truncated CI expansions. This introduces the lack of size-extensivity and the related lack of *dynamic correlation* due to highly excited configurations. These limitations may be partially avoided by exploiting the multireference (MR) CI methods. The MR CI (usually MR CISD) methods are particularly beneficial when handling a manifold of quasidegenerate electronic states, which is invariably the case when exploring the potential

energy surfaces or curves in the domain of geometries involving highly stretched or broken chemical bonds.

In fact, the MR methods are indispensable to handle the *static correlations* due to the degeneracy of the states considered and are likewise very efficient to account for *nondynamic correlations* arising in quasidegenerate situations. Yet, to account for dynamic correlation effects requires the use of CI spaces of very high dimensions. For this reason, one generally reverts to a *post hoc* account of the dynamic correlation and size-extensivity (usually *via* the low-order perturbation theory and various Davidson-type corrections).

The methods based on the *many-body perturbation theory* (MBPT) (*cf.* refs[8–10]) are in many aspects complementary to the variational approaches. In their Rayleigh–Schrödinger version, they are universally size-extensive at any level of truncation, but – at least in their single reference (SR) version – are unable to account for nondynamic correlations once the quasidegeneracy sets in. The finite-order MBPT methods are limited to the third, or at most the fourth, order in view of the rapidly increasing computational demands. Even though already the second-order results provide a wealth of useful information, and the fourth-order results are often sufficiently accurate, there are many instances when selective higher-than-fourth-order terms make a non-negligible contribution. This is the main reason for a widespread use of the coupled-cluster (CC) approaches[11–14] that exploit the exponential cluster Ansatz for the wave operator, thus enabling the summation of certain classes of the MBPT diagrams to an infinite order. This is automatically achieved by solving the energy-independent CC equations, which can be viewed as recursion formulas for the generation of higher-order MBPT contributions of a certain kind on the basis of the lower-order ones.

In many instances, such as the nondegenerate, closed-shell or high-spin open-shell ground states, it is adequate to truncate the CC expansion at the pair cluster level (CCSD approximation). To achieve the so-called chemical accuracy of ≈1 kcal/mol, at least a perturbative account of triples may be required *via* the CCSD(T) approach[15,16]. Needless to say that the full account of triples (and, of course, quadruples) is again computationally too demanding, except for small systems. Unfortunately, once the quasidegeneracy sets in, the importance of higher-than-pair clusters rapidly increases, causing the CCSD results to deteriorate, while CCSD(T) breaks down completely (*cf.*, *e.g.*, ref.[14]).

Although much work has been devoted to the MR CC approaches (for an overview, see ref.[17] and references therein), and two genuine *bona fide* methods (referred to, respectively, as the *valence-universal* or *Fock-space* and

state-universal or *Hilbert-space* approaches) have been developed, their practical exploitation is severely limited not only by the complexity of the required algorithms and codes, but also by various intrinsic impediments, such as the intruder state problem, multiplicity and genealogy of solutions, *etc.* (*cf.* ref.[17]). In any case, no general-purpose codes implementing genuine MR CC approaches are presently available and most researchers center their attention on the so-called *state-selective* or *state-specific* MR CC methods that focus on one state at a time (*cf.* also refs[18–21] and references therein). Such approaches are also the subject of this contribution.

BASIC FORMALISM AND NOTATION

In the standard SR CC method, the exact electronic wave function $|\Psi\rangle$, describing some nondegenerate, lowest-lying (for a given symmetry species) state, is represented *via* the so-called *cluster expansion* relative to some IPM state $|\Phi_0\rangle$ that represents a reasonable approximation to $|\Psi\rangle$ (usually the RHF state). In other words, one employs the exponential cluster Ansatz for the wave operator W that transforms $|\Phi_0\rangle$ into $|\Psi\rangle$, $|\Psi\rangle = W|\Phi_0\rangle$, namely

$$|\Psi\rangle = e^T |\Phi_0\rangle , \qquad \langle\Phi_0|\Phi_0\rangle = \langle\Phi_0|\Psi\rangle = 1 , \tag{1}$$

where the cluster operator T is given by the sum of its n-body connected components T_n (*cf.* refs[11–14])

$$T = \sum_{n=1}^{N} T_n . \tag{2}$$

The n-body operators T_n are in turn represented *via* a linear combination of the n-fold excitation operators $G_i^{(n)}$ relative to $|\Phi_0\rangle$,

$$T_n = \sum_{i=1}^{M_n} t_i^{(n)} G_i^{(n)} , \tag{3}$$

where $t_i^{(n)}$ are the n-body connected cluster amplitudes defining T_n, while $|\Phi_i^{(n)}\rangle = G_i^{(n)}|\Phi_0\rangle$ are the n-times excited IPM states or configurations relative to $|\Phi_0\rangle$ (either spin-adapted or not) that span the M_n-dimensional n-times excited subspace of the N-electron space considered.

The exponential nature of the CC Ansatz for $|\Psi\rangle$, Eq. (*1*), implies the size-extensivity of the resulting formalism regardless the truncation level

employed, which is not the case when we employ the linear CI Ansatz for $|\Psi\rangle$, *i.e.*,

$$|\Psi\rangle = C|\Phi_0\rangle = \sum_{n=0}^{N} C_n |\Phi_0\rangle , \qquad C_0 = 1 \tag{4}$$

where we again employ the intermediate normalization for $|\Psi\rangle$ and where the n-th order excitation operators C_n are similarly represented as in Eq. (*3*) with $t_i^{(n)}$ replaced by the CI coefficients $c_i^{(n)}$.

Comparing both expansions, Eqs (*1*) and (*4*), we easily find the relationship between the CI excitation operators C_n and the corresponding cluster operators T_n, namely

$$C_n = T_n + \sum_{\mathcal{P}_n} \left(\prod_{i=1}^{p} (n_i!)^{-1} T_i^{n_i} \right), \tag{5}$$

where the sum extends over all nontrivial, distinct partitions $\mathcal{P}_n$ of n, $\mathcal{P}_n \equiv \{1^{n_1} 2^{n_2} \ldots n^{n_n}\}$, $n = \sum_{i=1}^{p} i n_i$, $0 \le n_i \le n$, $1 \le p < n$, or, explicitly,

$$\begin{aligned} C_1 &= T_1 \\ C_2 &= T_2 + \tfrac{1}{2} T_1^2 \\ C_3 &= T_3 + T_1 T_2 + \tfrac{1}{6} T_1^3 \\ C_4 &= T_4 + \tfrac{1}{2} T_2^2 + T_1 T_3 + \tfrac{1}{2} T_1^2 T_2 + \tfrac{1}{24} T_1^4 , \quad \textit{etc.} \end{aligned} \tag{6}$$

Thus, each higher-than-one-body CI excitation operator C_n consists of the connected cluster component T_n of the same order, as well as of the disconnected component(s) involving products of the lower-order cluster operators.

The CI, and particularly the CC Ansätze considerably simplify when we employ the maximum overlap or Brueckner orbitals, in which case the monoexcited components vanish, *i.e.*,

$$C_1 = T_1 = 0 , \tag{7}$$

so that $C_2 = T_2$, $C_3 = T_3$, and the first disconnected component appears at the quadruply-excited level,

$$C_4 = T_4 + \tfrac{1}{2} T_2^2 \tag{8}$$

Now, the pair clusters represent generally the most important contribution to T and in the absence of quasidegeneracy are responsible for 94–96% of the correlation energy. In fact, when Eq. (*7*) holds, only the pair clusters T_2 directly contribute to the energy. The next important contribution, amounting to about 1–3% of the correlation energy, is due to the triples, while quadruples (and singles when not using the Brueckner orbitals) contribute only about 1% or less. Moreover, while the quadruple contribution is almost entirely due to the disconnected $\frac{1}{2} T_2^2$ clusters, the triple contribution is mainly due to the connected T_3 component, as first shown in ref.[22] Thus, in nondegenerate situations, the approximation $T \approx T_2$ (CCD method) or $T \approx T_1 + T_2$ (CCSD method) yields very good results and, in order to achieve chemical accuracy, one can account for T_3 perturbatively *via* CCSD(T). Once the quasidegeneracy sets in, however, the importance of the connected, higher-than-pair clusters (*i.e.*, T_3, T_4, *etc.*) increases, and we can no longer neglect these clusters or even treat them perturbatively.

In contrast to variational CI method, the cluster amplitudes $t_i^{(n)}$ (or, simply, t_i) are determined by solving a set of energy-independent CC equations that are obtained by suitably projecting the Schrödinger equation $H|\Psi\rangle = E|\Psi\rangle$, premultiplied with the inverse of W, onto the excited state manifold $\{|\Phi_i^{(n)}\rangle\}$, *i.e.*,

$$\langle \Phi_i^{(n)} | e^{-T} H e^{T} | \Phi_0 \rangle = 0 , \qquad (n = 1, \ldots, N;\ i = 1, \ldots, M_n) \tag{9}$$

while the energy is obtained by projecting onto the reference $|\Phi_0\rangle$,

$$E = \langle \Phi_0 | e^{-T} H e^{T} | \Phi_0 \rangle = \langle \Phi_0 | H e^{T} | \Phi_0 \rangle , \tag{10}$$

so that

$$\Delta E = E - \langle \Phi_0 | H | \Phi_0 \rangle = \langle \Phi_0 | H (T_1 + T_2 + \tfrac{1}{2} T_1^2) | \Phi_0 \rangle \tag{11}$$

represents the correlation energy assuming that $|\Psi_0\rangle$ is a HF reference (*cf.*, *e.g.*, ref.[14]). Note that, in general, the energy E is given by the asymmetric energy formula

$$E = \langle \Xi | H | \Psi \rangle / \langle \Xi | \Psi \rangle , \qquad (12)$$

where $|\Xi\rangle$ represents any state that is not orthogonal to $|\Psi\rangle$. Clearly, in the present case, the expression for the energy E, Eq. (*12*), takes the form of Eq. (*10*) when we set $|\Xi\rangle = |\Phi_0\rangle$ and use the cluster Ansatz, Eq. (*1*), for $|\Psi\rangle$.

Now, similarly as in the CI case, Eq. (*9*) represents the chain of CC equations for $n = 1, 2, \ldots, N$. Since the disconnected terms do not contribute (*cf.* refs[14,17]), so that

$$\langle \Phi_i^{(n)} | e^{-T} H e^{T} | \Phi_0 \rangle = \langle \Phi_i^{(n)} | H e^{T} | \Phi_0 \rangle_C = 0 , \quad (n = 1, \ldots, N;\ i = 1, \ldots, M_n) \qquad (13)$$

where the subscript C implies that only connected terms are to be retained, the CC chain of equations takes the form

$$\begin{aligned}
&\langle \Phi_i^{(1)} | H[1 + T_1 + (T_2 + \tfrac{1}{2} T_1^2) + (T_3 + T_1 T_2 + \tfrac{1}{6} T_1^3)] | \Phi_0 \rangle_C = 0 , \\
&\langle \Phi_i^{(2)} | H[1 + T_1 + (T_2 + \tfrac{1}{2} T_1^2) + (T_3 + T_1 T_2 + \tfrac{1}{6} T_1^3) + \\
&\qquad + (T_4 + T_1 T_3 + \tfrac{1}{2} T_1^2 T_2 + \tfrac{1}{24} T_1^4)] | \Phi_0 \rangle_C = 0 , \\
&\langle \Phi_i^{(3)} | H[1 + T_1 + (T_2 + \tfrac{1}{2} T_1^2) + \ldots + (T_5 + T_1 T_4 + \ldots)] | \Phi_0 \rangle_C = 0 , \quad \textit{etc.}
\end{aligned} \qquad (14)$$

This chain is closely related to the corresponding CI chain

$$\begin{aligned}
&\langle \Phi_i^{(n)} | H(C_{n-2} + C_{n-1} + C_n + C_{n+1} + C_{n+2}) | \Phi_0 \rangle = E \langle \Phi_i^{(n)} | C_n | \Phi_0 \rangle , \\
&\qquad (n = 1, \ldots, N;\ i = 1, \ldots, M_n)
\end{aligned} \qquad (15)$$

where $C_n = 0$ if $n < 0$ or $n > N$. Indeed, replacing C_n by their CC equivalents, Eq. (*6*), and realizing that the disconnected terms on the left-hand side of Eq. (*15*) are exactly canceled by the right-hand-side energy-dependent term (*cf.* ref.[23] for details), we obtain the CC chain, Eq. (*14*). Clearly, without the truncation, both chains are equivalent, so that the full CI (FCI) and FCC both represent the exact solution for a given finite-dimensional *ab initio* model.

Unfortunately, FCI or FCC can only be carried out for relatively small model systems and in most actual applications one has to rely on truncated

schemes. This is done by simply decoupling the full CI or CC chain at a given excitation level, say m, by neglecting the higher-order terms, *i.e.*, by setting $C_{m+1} = C_{m+2} = 0$ or $T_{m+1} = T_{m+2} = 0$. When $m = 2$, we get the ubiquitous CISD or CCSD methods, respectively. In the former case, we diagonalize the corresponding principal submatrix of the FCI matrix, while in the latter case, we solve a nonlinear and nonhomogeneous algebraic system of equations of the type

$$a_i + \sum_j b_{ij}\, t_j + \sum_{j<k} c_{ijk}\, t_j\, t_k + \ldots = 0\ , \qquad (16)$$

and subsequently evaluate the energy by using the one- and two-body amplitudes in Eq. (*10*) or (*11*).

As already pointed out, CCSD provides an excellent approximation, which can be further improved by a perturbative account of triples. Unfortunately, when the state considered becomes quasidegenerate, as is invariably the case when considering stretched geometries or when breaking true chemical bonds, the higher-than-pair clusters start to play an important role and their perturbative account breaks down. Thus, CCSD(T) becomes entirely inadequate even when CCSD still performs reasonably well (*cf.*, *e.g.*, ref.[14]). Moreover, when we dissociate multiple bonds, say the triple bond in the N_2 molecule, even the hexuples are required for a proper description.

It should be noted that the inadequate performance of CCSD when breaking chemical bonds stems from the lack of size-consistency of the RHF, or generally IPM, reference. It is well known that even when breaking a single bond, say in the H_2 molecule, the RHF wave function tends to a wrong dissociation limit involving a mixture of covalent and ionic states. In many cases, one can employ an unrestricted HF (UHF) wave function [of the different-orbitals-for-different-spins (DODS) type] to achieve the correct dissociation. Unfortunately, this solution is hardly satisfactory when we wish to generate entire potential energy surfaces or curves, since the UHF solution generally exists only within a limited range of geometries, so that the resulting potentials are nonanalytic at the onset of the singlet-triplet instability (*cf.* ref.[24]), not to mention other shortcomings of such broken-spin-symmetry wave functions (*cf.* ref.[14]).

Although a proper account of both dynamic and nondynamic correlations in the presence of the quasidegeneracy can only be achieved by relying on genuine MR descriptions, much can be achieved to extend the

validity and usefulness of the SR CCSD method by relying on the state-selective or state-specific MR CC approaches. Here also belong the *externally corrected* CCSD (ecCCSD) methods which we consider next.

EXTERNALLY CORRECTED CCSD METHODS

Since the CCSD method is well suited for the description of dynamic correlation effects, while in the presence of quasidegeneracy it fails to account for nondynamic correlations – which in turn is reflected in the increased role played by the T_3 and T_4 clusters – the basic idea of ecCCSD approaches is to exploit some independent source of information concerning these clusters. Such a source must efficiently describe the nondynamic correlation and be size-consistent, while being easily accessible without an undue computational effort.

The first attempt in this direction was undertaken a long time ago[25] and exploited, at least implicitly, the UHF wave function. More recently, an explicit use of the UHF wave function was studied[26]. Even though both approaches provide a greatly improved description in many situations (see also ref.[14] and references therein), the most serious shortcoming of the UHF source is the complete lack of the T_3 clusters[25,26].

More recently, we have exploited valence-bond (VB) type wave functions in ecCCSD approaches with a considerable success[27]. Unfortunately, we were able to carry out this study only at the semiempirical level due to the lack of suitable *ab initio* VB codes. For this reason we also examined the possibilities offered by the complete active space (CAS) self-consistent field (SCF) or CAS FCI wave functions[28,29], the option also suggested by Stolarczyk[30]. All these attempts proved to be very promising, particularly for open-shell systems, in which case we have employed the fully spin-adapted CCSD method that is based on the unitary group approach (UGA)[14,31]. Nonetheless, by far the most useful external source turned out to be a modest-size MR CISD wave function that is based on an M-dimensional reference space. This led us to design the amplitude-corrected, reduced MR (RMR) CCSD method[14,32–39] and, most recently, the energy-corrected CCSD-[MR] method[40–44]. The latter approach was stimulated by the work of Piecuch and Kowalski[45,46] on the *method of moments*[45,47], leading to the MBPT-based *renormalized* and *completely renormalized* CCSD(T) methods[46,48]. In the following, we focus only on the MR CISD-based methods.

The main reasons for the utility of the MR CISD wave function as the external source for the ecCCSD methods may be summarized as follows:

1. There is a definite complementarity between the SR CCSD and MR CISD wave functions in their ability to account for, respectively, the dynamic and nondynamic correlations, as already alluded to above.

2. The MR CISD wave function can be easily re-expressed in the SR CI form (relative to the RHF reference $|\Phi_0\rangle$) involving higher-than-pair excitations.

3. There is a simple and well-defined relationship between the SR CC and SR CI Ansätze, as given by Eq. (*5*) or (*6*).

4. By extracting the three- and four-body, connected, cluster amplitudes, we automatically account for all higher-than-quadruply-excited (relative to $|\Phi_0\rangle$) configurations that are present in the MR CISD wave function.

5. A modest-size MR CISD wave function (M = 2 to 8) contains only a very small subset of the three- and four-body amplitudes.

6. Finally, in the $m \rightarrow N$ limit, we reach the FCI and FCC methods, both yielding the same state and the same energy.

The MR CISD wave function that we usually employ is designed to properly achieve the size-consistency for the considered dissociation channel at the minimum cost. This implies that we choose as small as possible reference space. Thus, for example, to dissociate a single bond, we need at least two active orbitals (typically represented by the highest occupied and lowest unoccupied molecular orbitals, *i.e.*, by HOMO and LUMO) for the two electrons, implying at most a four-dimensional reference space (depending on the symmetry of HOMO and LUMO and the spin-adaptation employed). In the challenging case of a triple-bond dissociation, we need generally to distribute 6 electrons over 6 orbitals. In the singlet case with no spatial symmetry present this implies already a 175-dimensional reference space. However, we have shown[34] that we can do with much smaller reference spaces: For example, in the case of the nitrogen molecule dissociation, an eight-dimensional reference space is quite adequate[37].

We next outline two distinct ways of exploiting the MR CISD wave function for the correcting of the standard SR CCSD method.

Amplitude-Corrected CCSD

The basic impetus for this type of ecCCSD stems from the fact that the CCSD approximation arises by the decoupling of the singly- and doubly-projected set of CC equations from the rest of the full CC chain by neglecting the T_3 and T_4 clusters, *i.e.*, by setting

$$T_3 = T_4 = 0 \qquad (17)$$

in Eqs (*14*). Such a decoupling is, of course, possible due to the fact that our Hamiltonian involves at most two-body terms, so that doubles can interact with at most quadruples. Thus, were we able to obtain the exact three- and four-body cluster amplitudes, the CCSD decoupling could be made exact. Indeed, using, for example, the T_3 and T_4 clusters that result from the cluster analysis of the FCI wave function, and evaluating the T_3- and T_4-dependent terms in the first and the second equations in the CC chain (*14*), we obtain formally the CCSD equations whose solution will return the exact T_1 and T_2 clusters, and thus the exact energy. Actually, we use this fact to test our codes.

Now, once the quasidegeneracy sets in, the T_3 and T_4 clusters gain in importance, so that when we use even the approximate values for the most important three- and four-body cluster amplitudes, we achieve a superior approximation to the standard SR CCSD method, in which these clusters are completely neglected, Eq. (*17*). In other words, we employ the CC Ansatz, Eq. (*1*), with

$$T \approx T_1 + T_2 + T_3^{(0)} + T_4^{(0)} , \qquad (18)$$

where $T_n^{(0)}$, n = 3, 4 represent some *a priori* fixed approximation to T_n, n = 3, 4. In the RMR CCSD method, it is a modest-size MR CISD wave function that is used for this purpose: Expressing formally this wave function as a SR CI Ansatz (relative to the reference $|\Phi_0\rangle$), we carry out the cluster analysis yielding the $T_3^{(0)}$ and $T_4^{(0)}$ clusters. We then evaluate, once and for all, the terms to which these 3- and 4-body clusters contribute and correct accordingly the CCSD equations, which have again formally the same form as the standard CCSD equations, except for the actual values of the coefficients a_i and b_{ij}, Eq. (*16*).

Strictly speaking, the $\langle \Phi_i^{(1)} | H T_3^{(0)} | \Phi_0 \rangle_C$ and $\langle \Phi_i^{(2)} | H T_n^{(0)} | \Phi_0 \rangle_C$, n = 3, 4 terms are added to the absolute term a_i, Eq. (*16*), while the $\langle \Phi_i^{(2)} | H T_1 T_3^{(0)} | \Phi_0 \rangle_C$ terms contribute to the linear b_{ij} coefficients, Eq. (*16*). However, since these latter terms are generally less important (being entirely absent when the Brueckner orbitals are employed), we can replace them by the terms $\langle \Phi_i^{(2)} | H T_1^{(0)} T_3^{(0)} | \Phi_0 \rangle_C$, using the approximate $T_1^{(0)}$ clusters that are a byproduct of the cluster analysis of the MR CISD wave function. In this way, we

only have to correct the absolute terms a_i, Eq. (*16*), and deal with a much simpler algorithm without hardly influencing the result[27–29].

We can also view the amplitude-corrected ecCCSD method as an approximation to the CCSDTQ method, in which we set initially $T_n = T_n^{(0)}$ for $n = 3$ and 4, thus reducing it effectively to CCSD. Note however, that while ecCCSD is capable of yielding, in principle, the exact FCI or FCC result (assuming that we use exact T_n clusters for $T_n^{(0)}$, $n = 3, 4$), this is never possible by solving CCSDTQ equations (unless we deal, of course, with a 4-electron system when CCSDTQ is equivalent to FCC). In other words, the MR CISD-based three- and four-body cluster amplitudes have implicitly "built into" them higher-than-four-body effects, as long as these are present in the MR CISD wave function. For example, when using a minimal eight-dimensional reference space in the case of the N_2 molecule[34,37], we automatically account even for the most important hexuply-excited terms.

The above remark could make the impression that we initially require one iteration of the CCSDTQ method. However, this is not the case, since the three- and four-body amplitudes that result by the cluster analysis of a typical MR CISD wave function form only a very small subset of all triples and quadruples. For example, when breaking a single bond and using an active space involving HOMO and LUMO, say σ and σ* MOs, we deal with a two-dimensional reference space (assuming that σ and σ* belong to different symmetry species) that is spanned by the ground state configuration $|\Phi_0\rangle = |\{...\sigma^2\}\rangle$ and the biexcited (relative to $|\Phi_0\rangle$) configuration $|\Phi_1\rangle = |\{...(\sigma^*)^2\}\rangle$, where we list explicitly only the active orbitals. The corresponding MR CISD wave function, when expressed in the SR CISDTQ form relative to $|\Phi_0\rangle$, involves quadruples that are doubles relative to $|\Phi_1\rangle$. Now, the number of these quadruples is approximately the same as the number of doubles (relative to $|\Phi_0\rangle$), *i.e.*, considerably less than is the total number of quadruples. Likewise, even when larger reference spaces are employed, the number of three- and four-body cluster amplitudes is much smaller than is the dimension of the respective triply- and quadruply-excited components of the relevant *N*-electron space.

Energy-Corrected CCSD

The above outlined RMR CCSD method represents an ecCCSD approach that results by modifying the standard CCSD equations *via* a noniterative incorporation of the T_3- and T_4-dependent terms, using the three- and four-body cluster amplitudes extracted from the MR CISD wave function *via* the cluster analysis. This incorporates the MR effects and ascertains a

more physical decoupling of the CC chain of equations at the CCSD level than does a simple neglect of the T_3 and T_4 clusters. By solving these corrected CCSD equations, we obtain more reliable T_1 and T_2 clusters and thus more precise energy. Hence the term *amplitude-corrected* approaches in contrast to those methods that rely on the standard SR CCSD amplitudes, such as CCSD(T), and which we refer to as the *energy-corrected* methods [in the CCSD(T) case, *internally* energy-corrected methods, since no external source is employed]. This latter type of approaches received a new impetus thanks to the above quoted developments by Piecuch and Kowalski[45,46,48] (for the relationship with the so-called *variational* and *extended* CC theories, see ref.[49]). For our purposes, the essence, as well as the required formalism, of the MR-CISD-based energy-corrected CCSD method is most easily described by relying on the asymmetric energy formula, Eq. (*12*).

Note that Eq. (*12*) yields the exact energy when either $|\Psi\rangle$ or $|\Xi\rangle$ are exact and incorporates both the CI and CC energy expressions as a special case[40,42]. In the CC case, one sets $|\Xi\rangle \equiv |\Phi_0\rangle$, Eq. (*10*) or (*11*). Yet, it is important to realize that the same energy is obtained when $|\Xi\rangle$ involves, in addition to $|\Phi_0\rangle$, any of the configurations $|\Phi_i^{(n)}\rangle$ that define the truncated CC scheme employed, since all such terms vanish in view of Eq. (*13*). Only higher-excited configurations (in the CCSD case those with $n > 2$) will generate nonvanishing contributions to E. This was clearly shown by Piecuch *et al.*[46,48], who exploited the MBPT-type wave function for $|\Xi\rangle$ to define their renormalized methods that efficiently correct the pathological behavior of the above mentioned standard CCSD(T).

Our results obtained with the RMR CCSD method[32–34,36–39] imply that an efficient way to incorporate the absent nondynamic correlation effects into the standard CCSD formalism is to rely on a suitable MR CISD wave function. We have thus examined the results provided by the asymmetric energy formula, Eq. (*12*), using the standard CCSD wave function for $|\Psi\rangle$, $|\Psi\rangle \approx |\Psi^{(\mathrm{CCSD})}\rangle$, and various MR CISD wave functions for $|\Xi\rangle$. Interestingly enough, we have often obtained in many cases practically the same results as with the RMR CCSD method, using, of course, the same MR CISD wave function in each case. Even better results are obtained when we employ an RMR CCSD wave function for $|\Psi\rangle$ [40], although this step significantly increases the computational cost.

The complementarity of the CI and CC approaches in handling of dynamic and nondynamic correlations is also corroborated by the fact that the energy obtained *via* the asymmetric energy formula, Eq. (*12*), can be interpreted as either the CC (*i.e.*, CCSD) energy plus the CI (*i.e.*, MR CISD) correction or as the CI energy plus the CC-based correction[40,42]. Indeed, us-

ing the CCSD (or, in fact, RMR CCSD) wave function for $|\Psi\rangle$ and the resolution of the identity in Eq. (*12*), we easily find[40] that (*cf.* also refs[46,48])

$$E = E^{(\mathrm{CC})} + \Delta E^{(\mathrm{CC})} , \tag{19}$$

where

$$\begin{aligned} \Delta E^{(\mathrm{CC})} &= N \sum_{n>2} \sum_{i} \langle \Xi | e^{T} | \Phi_i^{(n)} \rangle \langle \Phi_i^{(n)} | e^{-T} H e^{T} | \Phi_0 \rangle , \\ N &= \langle \Xi | e^{T} | \Phi_0 \rangle^{-1} . \end{aligned} \tag{20}$$

Here $E^{(\mathrm{CC})}$ represents the CCSD (or RMR CCSD) energy and the sum extends over all higher-than-doubly-excited configurations that are present in the MR CISD wave function.

Focusing, instead, on a CI (*i.e.*, MR CISD) wave function $|\Xi\rangle$, which we simply represent in the form

$$|\Xi\rangle = \sum_{\Phi_i \in \mathcal{M}} c_i |\Phi_i\rangle , \tag{21}$$

where $\mathcal{M}$ designates the relevant CI subspace of the chosen N-electron space $\mathcal{W}$, $\mathcal{M} = \mathrm{Span}\{|\Phi_i\rangle\} \subset \mathcal{W}$, we have that

$$H|\Xi\rangle = E^{(\mathrm{CI})}|\Xi\rangle + \sum_{\Phi_i \in \mathcal{M}^{\perp}} |\Phi_i\rangle\langle\Phi_i|H|\Xi\rangle , \tag{22}$$

where $\mathcal{M}^{\perp}$ is the orthogonal complement of $\mathcal{M}$ in $\mathcal{W}$. It easily follows[40] that

$$E = E^{(\mathrm{CI})} + \Delta E^{(\mathrm{CI})} , \tag{23}$$

where

$$\Delta E^{(\mathrm{CI})} = N \sum_{\Phi_i \in \mathcal{M}^{(\mathrm{IS})}} \langle \Xi | H | \Phi_i \rangle \langle \Phi_i | e^{T} | \Phi_0 \rangle , \tag{24}$$

with $\mathcal{M}^{(\mathrm{IS})} \subset \mathcal{M}^{\perp}$ designating the first-order interacting space of $\mathcal{M}$. The correction $\Delta E^{(\mathrm{CI})}$ may thus be regarded as the CC-based Davidson-type correc-

tion and, in fact, may be interpreted as the second-order PT correction to $E^{(CI)}$ (ref.[40]).

ILLUSTRATIVE EXAMPLES

Both the RMR CCSD and the energy-corrected CCSD methods have been thoroughly tested on various model systems[32–44], including a challenging problem of the triple-bond breaking as exemplified by the dissociation of the N_2 molecule[37,40]. Here we wish to illustrate the performance and capabilities of these approaches by presenting some typical results concerning the ground-state spectroscopic properties of two first-row hydrides, namely the LiH and HF molecules. These molecules have been the subject of numerous experimental and theoretical studies (*cf.* also refs[33,43,44]) and the ground states of their most important isotopomers have been well characterized by various spectroscopic techniques[50–56]. The comparison of the experimental and computed ro-vibrational energy levels and transition frequencies constitutes an ultimate test for any theoretical method, since even very small energy changes in the computed energy may lead to significant errors in the spectral characteristics, particularly for high-lying levels near the dissociation threshold.

Computational Details and Acronyms

For the single-bonded LiH and HF molecules, the MR effects arise near the dissociation limit due to the orbital degeneracy of the σ bonding and σ* antibonding MOs. Hence we use a four-dimensional model space $\mathcal{M}$ for the required MR CISD. This space is spanned by the Hartree–Fock reference $|\Phi_0\rangle = |\{..., \sigma\alpha, \sigma\beta\}\rangle$, two singly-excited configurations $|\Phi_1\rangle = |\{..., \sigma^*\alpha, \sigma\beta\}\rangle$, and $|\Phi_2\rangle = |\{..., \sigma\alpha, \sigma^*\beta\}\rangle$, and one doubly excited configuration $|\Phi_3\rangle = |\{..., \sigma^*\alpha, \sigma^*\beta\}\rangle$.

Generally, a reference space involving M configurations is referred to as the MR space, and the MR CISD method employing this reference space as MR-CISD. Clearly, in our case $M = 4$. The RMR CCSD method that employs MR-CISD wave function is characterized by the acronym MR-RMR CCSD, or MR-RMR for short, and the corresponding energy-corrected CCSD method by CCSD-[MR].

In all our calculations we employ correlation-consistent (cc), polarized, Cartesian cc-pVXZ basis sets of Dunning *et al.*[57,58], where X = D, T, and Q characterize, respectively, a double-, triple-, and quadruple-zeta basis. The Hartree–Fock MOs, and the required one- and two-electron integrals, have been generated with the GAMESS[59] package, while all CI and CC results

were obtained with our own codes. The ro-vibrational energy levels $E(v, J)$ associated with the vibrational quantum number v and the rotational quantum number J have been generated *via* the numerical integration of the radial Schrödinger equation for the nuclear motion using our theoretically determined potentials and the LEVEL codes of LeRoy[60].

Spectroscopy of the LiH Ground State

We focus here on the LiH molecule for the following reasons:

1. For this small four-electron system, we can generate the FCI results even for a relatively sizable basis set of a triple-zeta quality (cc-pVTZ). This should enable us to assess the relative sizes of the errors due to the approximations inherent in the method employed *vs* those due to the basis set limitations.

2. New, highly-precise spectroscopic data have been recently generated for this system and its various isotopomers[52]. Here we present a few typical results and the full treatment will appear elsewhere[44].

3. To explore the role of the core-correlation effects, we shall examine the first-row hydrides from both ends of the periodic table. The results for the HF molecule, obtained with the frozen fluorine core, have been extensively studied earlier[43].

Let us first consider the FCI results obtained with the cc-pVTZ basis set[58], representing the exact result for this model, and compare them with those obtained by approximate CI and CC approaches, as well as with the experiment. The FCI/cc-pVTZ energies for 41 geometries that define the potential energy curve (PEC) employed are listed in Table I (*cf.* also Table I of ref.[44]). This PEC is compared with the CCSD, 4R-CISD, and CCSD-[4R] PECs, obtained with the same basis set, in Fig. 1. (The 4R-RMR PEC is not shown, since on the scale of the figure it coincides with the CCSD-[4R] PEC.)

We see from Fig. 1 that only the 4R-CISD potential substantially deviates from the FCI one once the internuclear separation R increases beyond $1.5R_e$ or $2R_e$, where R_e designates the equilibrium bond length. Indeed, in the vicinity of the equilibrium geometry, $R = R_e$, all four PECs practically coincide, implying that we have to consider the entire range of geometries in order to properly assess the performance of a given method. (Note that all the potentials shown in Fig. 1 are shifted on the energy scale in order to coincide at $R = R_e$.)

A very sensitive test is then provided by the computed vibrational energy levels that are also shown in Fig. 1. We see that even the standard CCSD method performs very well in this case and significant differences relative

to the exact FCI values occur only for high-lying levels. Indeed, the difference between the FCI and CCSD vibrational energy levels amounts to less than 1 cm^{-1} for levels up to and including $\nu = 3$ and less than 10 cm^{-1} up to $\nu = 11$, but then steadily rises to about 150 cm^{-1} for the highest, $\nu = 22$, level. Remarkably enough, both 4R-RMR and CCSD-[4R] errors are considerably smaller, being below 1 cm^{-1} for the first six levels, below 10 cm^{-1} up to $\nu = 15$, and reaching the maximum deviation of 23 to 24 cm^{-1} for the topmost $\nu = 22$ level, *i.e.*, about six times smaller error than the CCSD one.

Interestingly enough, the 4R-CISD results are least accurate, slightly exceeding the 1 cm^{-1} error even for the $\nu = 0$ level and eventually reaching an almost 400 cm^{-1} error for $\nu = 21$, which represents the highest-lying level for this potential. It is thus noteworthy that the MR CISD method, which provides us with the three- and four-body cluster amplitudes that significantly improve the performance of the standard CCSD method in the quasidegenerate region, performs itself so poorly. This deficiency must clearly be ascribed to its inability to properly account for the dynamic correlation effects.

TABLE I
The FCI total energy *E* of LiH, obtained with the cc-pVTZ basis set, as a function of the internuclear separation *R*

R, Å	*E*, a.u.	*R*, Å	*E*, a.u.	*R*, Å	*E*, a.u.
1.0	–7.945930	2.4	–8.006381	3.8	–7.956245
1.1	–7.984079	2.5	–8.001057	3.9	–7.954950
1.2	–8.009188	2.6	–7.995880	4.0	–7.953875
1.3	–8.025048	2.7	–7.990902	4.1	–7.952988
1.4	–8.034310	2.8	–7.986164	4.2	–7.952259
1.5	–8.038850	2.9	–7.981700	4.5	–7.950785
1.6	–8.040025	3.0	–7.977536	4.7	–7.950204
1.7	–8.038837	3.1	–7.973693	5.0	–7.949684
1.8	–8.036026	3.2	–7.970188	5.2	–7.949481
1.9	–8.032129	3.3	–7.967030	5.5	–7.949299
2.0	–8.027525	3.4	–7.964221	5.7	–7.949228
2.1	–8.022482	3.5	–7.961755	6.0	–7.949164
2.2	–8.017189	3.6	–7.959619	6.6	–7.949109
2.3	–8.011786	3.7	–7.957791		

Now, the cc-pVTZ basis set is sufficiently large to allow a meaningful comparison with the experiment. Such a comparison is shown in Fig. 2, which displays the experimental PEC (ref.[50]), derived *via* the inverted perturbative approach (IPA) (*cf.* refs[61–63]), together with the FCI/cc-pVTZ PEC of Fig. 1, the CCSD-[4R] PEC corresponding to the complete basis set (cbs) limit obtained *via* the extrapolation procedure of Peterson and Dunning, Jr.[64] applied to the CCSD-[4R]/cc-pVXZ PECs for X = D, T, and Q basis sets, and the CCSD-[4R]/cc-pVQZ PEC including the adiabatic corrections for the H atom[50] (*cf.* ref.[44] for details). We immediately observe that it is the FCI/cc-pVTZ potential, and the corresponding vibrational energy levels, that deviate most from the experimentally determined values. Quantitatively, these deviations steadily increase to about 66 cm^{-1} at $v = 13$ and 14, and then rapidly decrease to –230 cm^{-1} at $v = 22$, passing through zero between $v = 18$ and $v = 19$. Clearly, the 4R-RMR/cc-pVTZ or CCSD-[4R]/cc-pVTZ results (that are not included in Fig. 2) behave in a very similar way as the FCI data (see Fig. 1). On the other hand, the CCSD-[4R] results obtained with the cc-pVQZ basis set (*cf.* ref.[44]), or even slightly better results, shown in Fig. 2, that are obtained when we add the empirically determined adiabatic corrections to our PEC (average deviation amounting to ≈16 cm^{-1} and, with the

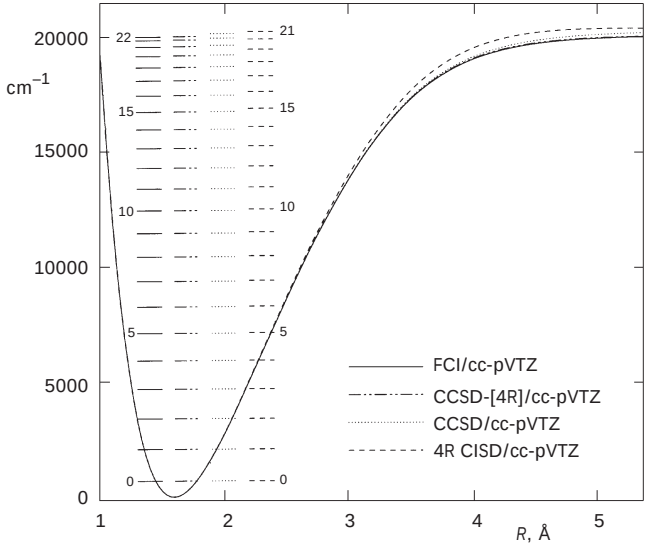

FIG. 1
Potential energy curves obtained with the FCI, CCSD, 4R-CISD, and CCSD-[4R] methods using the cc-pVTZ basis set, and the corresponding vibrational energy levels

exception of the topmost level, the maximum deviation to ≈30 cm^{-1}), as well as those obtained with the potential that has been extrapolated to the cbs limit (average deviation being 12.5 cm^{-1} and the maximal one ≈24 cm^{-1}), agree extremely well with experiment.

These results, together with those shown in Fig. 1, imply that at the cc-pVTZ level the basis set errors significantly exceed those due to the approximations that are involved in either the 4R-RMR or CCSD-[4R] methods, both yielding almost identical results. Indeed, at the cc-pVTZ level, the average deviation of the 4R-RMR or CCSD-[4R] vibrational term values from the FCI ones is less than 9 cm^{-1}, while the discrepancy between the FCI and experiment is on average ≈52 cm^{-1}. Once we improve the basis set to either the cc-pVQZ or cbs level, we greatly improve the agreement with experiment. Note also that the adiabatic corrections are relatively modest and amount to only a few wave numbers (on average to ≈3 cm^{-1}), the largest correction being again for the topmost $v = 22$ level (≈11 cm^{-1}).

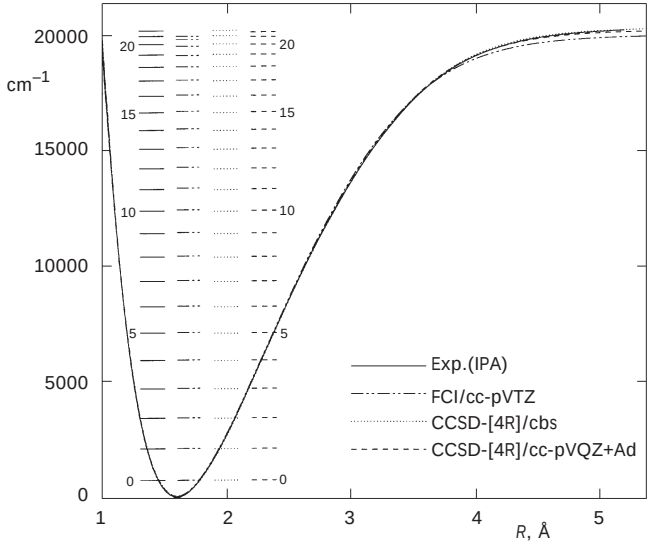

FIG. 2

The experimentally determined potential energy curve and the corresponding vibrational energy levels obtained *via* the IPA method[50] (solid curve and horizontal lines) and the corresponding theoretically derived data using the FCI/cc-pVTZ method, as well as the CCSD-[4R] method using either the complete basis set (cbs) limit extrapolation or the cc-pVQZ basis set and adiabatic corrections. The potentials are shifted on the energy scale so that the energy minimum corresponds to zero energy

It also should be pointed out that the extrapolation towards the cbs limit does not work as well for LiH as it does for larger systems (see, *e.g.*, the results for the HF molecule[43]). This is related to the fact that there is a very large difference between the double-zeta and triple-zeta potentials, and a much smaller one for a yet larger basis set. Nonetheless, we observe a typical pattern in the performance of the standard CCSD and ecCCSD methods, namely that the former method yields better agreement with experiment than the latter ones when small basis sets are employed, while the reverse holds once we increase the basis set size. In the LiH case, this is especially valid for the top few vibrational levels where the quasidegeneracy effects play the most significant role, as illustrated in Fig. 3, where we plot the discrepancies Δ_v between the computed and experimental vibrational term values G_v, $\Delta_v = G_v(\text{calc}) - G_v(\text{exp})$, as a function of the vibrational quantum number v, computed with the standard CCSD and 4R-RMR methods and the cc-pVXZ, X = D, T, and Q basis sets.

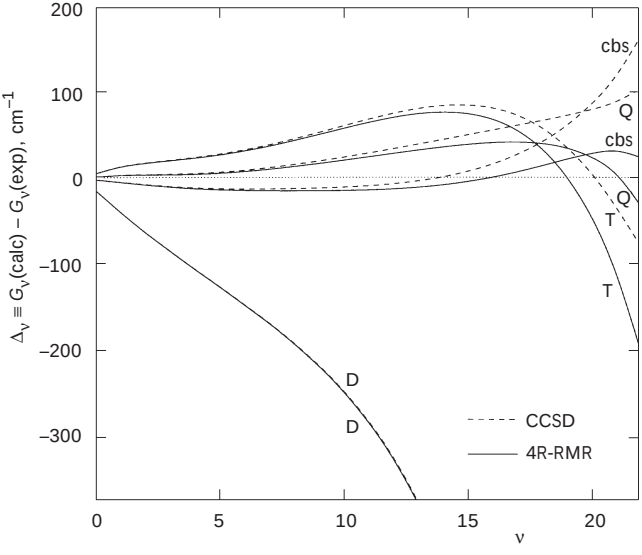

FIG. 3

Differences Δ_v between the calculated and experimental vibrational term values, $\Delta_v = G_v(\text{calc}) - G_v(\text{exp})$, as a function of the vibrational quantum number v, obtained with the standard CCSD (dashed lines) and 4R-RMR CCSD (solid lines) methods, using the cc-pVXZ, X = D, T and Q basis sets, as well as with the potential extrapolated to the complete basis set (cbs) limit

Other Isotopomers

In order to better assess the performance of ecCCSD approaches, we also present in Tables II and III the comparison of the experimentally determined[51,52] and computed vibrational energy levels for other isotopomers of ^{7}LiH, namely ^{7}LiD, ^{6}LiH, and ^{6}LiD. Table II lists the experimentally available vibrational term values G_v for the three isotopomers just mentioned and the deviations δ from the computed values using the CCSD-[4R] potential obtained with the cc-pVQZ basis set. We also included in this case the deviations δ_+ that result when we add adiabatic corrections[50] to the computed CCSD-[4R]/cc-pVQZ potential. We see that the effect of the adiabatic corrections is generally very small and becomes significant only for very high vibrational quantum numbers that approach the dissociation limit. We see again that the adiabatic corrections improve the agreement by about 2 cm^{-1} on average. Note that the differences from experiment amount on average to only 2–4 cm^{-1} for the first 10 vibrational levels.

Very similar results are provided by the 4R-RMR method as shown in Table III. Here we list only the results obtained with the potential including the adiabatic corrections and we also give the data for the standard ^{7}LiH isotope.

Transition Energies

The experimentally directly observed data are neither the PECs nor the vibrational term values, but the frequencies of spectral lines corresponding to the allowed transitions between ro-vibrational levels. Recently, Bernath's group measured hundreds of ro-vibrational lines for the isotopomers ^{6}LiH and ^{7}LiH, as well as for their deuterated analogues, with very high precision, using high-resolution Fourier-transform spectroscopy[52]. It is thus of interest to compare our computed spectra with these primary data. For obvious reasons we cannot present here the results for all the observed lines and all isotopomers. However, a few typical examples will amply illustrate the degree of agreement that can be achieved using the studied methods.

We only consider the main isotopic species, the ^{7}LiH molecule, since the results for other isotopomers are very similar, as already Tables II and III indicate. We have chosen the fundamental (1,0) vibrational band (Table IV), another $\Delta v = 1$ band associated with the largest vibrational quantum number observed, namely the (5,4) band (Table V), and finally, the strongest overtone (2,0) band (Table VI). In each case, we list the experimentally measured frequencies for all the observed lines in the *P* and *R* branches,

TABLE II

A comparison of the experimental[51] G_v(exp) and theoretical CCSD-[4R]/cc-pVQZ vibrational energy levels for three LiH isotopomers. The theoretical results are presented as deviations δ from the experimental values. The subscript "+" implies that the adiabatic corrections[50] were added to the computed potential. All values are in cm^{-1}

v	^{7}LiD			^{6}LiH			^{6}LiD		
	G_v(exp)	δ[a]	δ_+[b]	G_v(exp)	δ[a]	δ_+[b]	G_v(exp)	δ[a]	δ_+[b]
0	524.7	0.3	0.2	705.1	0.4	0.2	534.3	0.3	0.2
1	1553.7	1.8	1.5	2078.4	2.2	1.6	1581.8	1.8	1.5
2	2557.3	2.4	1.9	3406.1	2.8	1.7	2602.9	2.3	1.9
3	3535.9	2.5	1.8	4688.8	3.0	1.6	3598.0	2.4	1.8
4	4489.7	2.4	1.7	5927.6	3.6	1.7	4567.5	2.4	1.7
5	5419.1	2.6	1.7	7123.1	4.8	2.6	5511.8	2.6	1.7
6	6324.6	3.1	2.0	8276.2	6.7	4.2	6431.2	3.1	2.1
7	7206.4	3.9	2.7	9387.2	9.3	6.4	7326.2	4.1	2.9
8	8064.8	5.2	3.9	10456.6	12.4	9.1	8196.8	5.4	4.1
9	8900.0	6.8	5.3	11484.5	15.8	12.2	9043.5	7.1	5.6
10	9712.1	8.8	7.1	12471.0	19.5	15.5			
11	10501.3	10.9	9.1	13415.6	23.4	19.0			
12	11267.6	13.3	11.4	14317.7	27.3	22.5			
13	12011.1	15.9	13.8	15176.2	30.9	25.8			
14	12731.6	18.5	16.3	15989.1	34.2	28.7			
15	13428.9	21.3	18.9	16753.9	36.8	30.9			
16	14102.8	24.1	21.6	17466.6	38.3	31.9			
17	14752.7	26.9	24.2	18122.3	38.0	31.0			
18	15378.0	29.5	26.7	18713.9	35.0	27.4			
19	15978.0	31.9	29.0	19232.1	28.0	19.8			
20	16551.4	34.0	30.8	19664.5	15.0	6.0			
21	17096.8	35.5	32.2	19995.8	–8.1	–18.0			
22	17612.5	36.2	32.7						
23	18095.9	35.8	32.0						
24	18544.4	33.9	29.9						
25	18954.2	29.9	25.7						
26	19320.8	23.3	18.8						
27	19638.8	13.0	8.2						
$\lvert\delta_{10}\rvert_{av}$[c]		3.1	2.3		6.1	4.1		3.2	2.4
$\lvert\delta\rvert_{av}$[d]		16.9	14.7		18.0	14.4		3.2	2.4

[a] δ designates the deviation of the computed vibrational energy level obtained with the CCSD[4R]/cc-pVQZ potential from the experimental value. [b] δ_+ same as δ with the added adiabatic corrections. [c] Absolute average deviation for the first 10 vibrational levels. [d] Absolute average deviation for all levels.

TABLE III

A comparison of the experimental[51] G_v(exp) and theoretical 4R-RMR CCSD/cc-pVQZ vibrational energy levels with added adiabatic corrections for four LiH isotopomers. The theoretical results are presented as deviations δ_+ from the experimental values. All values are in cm^{-1}

v	^{7}LiH		^{7}LiD		^{6}LiH		^{6}LiD	
	G_v(exp)	δ_+[a]	G_v(exp)	δ_+[a]	G_v(exp)	δ_+[a]	G_v(exp)	δ_+[a]
0	697.9	0.2	524.7	0.2	705.1	0.2	534.3	0.2
1	2057.6	1.6	1553.7	1.5	2078.4	1.6	1581.8	1.5
2	3372.5	1.8	2557.3	1.9	3406.1	1.7	2602.9	1.9
3	4643.4	1.6	3535.9	1.9	4688.8	1.6	3598.0	1.9
4	5871.1	1.8	4489.7	1.7	5927.6	1.8	4567.5	1.7
5	7056.6	2.6	5419.1	1.7	7123.1	2.7	5511.8	1.8
6	8200.4	4.2	6324.6	2.1	8276.2	4.3	6431.2	2.1
7	9303.0	6.3	7206.4	2.8	9387.2	6.5	7326.2	3.0
8	10364.7	9.1	8064.8	4.0	10456.6	9.3	8196.8	4.2
9	11385.9	12.2	8900.0	5.5	11484.5	12.5	9043.5	5.8
10	12366.4	15.6	9712.1	7.3	12471.0	15.9		
11	13306.0	19.1	10501.3	9.4	13415.6	19.5		
12	14204.1	22.7	11267.6	11.7	14317.7	23.2		
13	15059.6	26.2	12011.1	14.1	15176.2	26.7		
14	15870.8	29.4	12731.6	16.8	15989.1	29.9		
15	16635.2	32.1	13428.9	19.5	16753.9	32.4		
16	17349.5	33.7	14102.8	22.2	17466.6	33.8		
17	18008.7	33.8	14752.7	25.0	18122.3	33.5		
18	18606.6	31.6	15378.0	27.6	18713.9	30.7		
19	19134.5	25.6	15978.0	30.1	19232.1	23.8		
20	19581.1	14.1	16551.4	32.2	19664.5	10.5		
21	19932.1	–6.9	17096.8	33.9	19995.8	–13.6		
22	20169.8	–45.1	17612.5	34.7				
23			18095.9	34.5				
24			18544.4	32.9				
25			18954.2	29.3				
26			19320.8	23.0				
27			19638.8	12.8				
$\lvert\delta_{10}\rvert_{av}$[b]		4.1		2.3		4.2		2.4
$\lvert\delta\rvert_{av}$[c]		16.4		15.7		15.3		2.4

[a] δ_+ designates the deviation of the computed vibrational energy level obtained with the CCSD[4R]/cc-pVQZ potential including the adiabatic correction[50] from the experimental value. [b] Absolute average deviation for the first 10 vibrational levels. [c] Absolute average deviation for all levels.

TABLE IV

The deviations of the computed transition frequencies from the experimentally (exp) observed ones[52] for the *P* and *R* lines of the (1,0) vibrational band of LiH, as obtained with the CCSD-[4R] method and the cc-pVXZ (X = D, T, and Q) basis sets. The subscript "+" indicates that the adiabatic corrections[50] were added to the potential. All values are in cm^{-1}

J	*P* branch					*R* branch				
	exp	D	T	Q	Q_+	exp	D	T	Q	Q_+
0						1374.1	–25.9	7.8	1.8	1.4
1	1344.9	–25.5	7.7	1.9	1.4	1388.0	–26.1	7.8	1.8	1.3
2	1329.7	–25.2	7.7	1.9	1.5	1401.5	–26.3	7.8	1.8	1.3
3	1314.1	–24.8	7.6	2.0	1.6	1414.5	–26.4	7.8	1.8	1.3
4	1298.1	–24.5	7.6	2.0	1.6	1427.0	–26.4	7.7	1.8	1.3
5	1281.8	–24.1	7.5	2.1	1.7	1439.0	–26.5	7.7	1.8	1.3
6	1265.2	–23.6	7.4	2.2	1.8	1450.4	–26.5	7.6	1.8	1.3
7	1248.3	–23.2	7.3	2.3	1.9	1461.3	–26.4	7.5	1.8	1.4
8	1231.1	–22.6	7.2	2.4	2.0	1471.6	–26.4	7.5	1.9	1.4
9	1213.6	–22.1	7.1	2.5	2.1	1481.3	–26.3	7.3	1.9	1.4
10	1195.9	–21.5	6.9	2.6	2.2	1490.4	–26.1	7.2	2.0	1.5
11	1178.0	–20.9	6.7	2.7	2.4	1499.0	–25.9	7.1	2.0	1.5
12	1159.9	–20.3	6.5	2.8	2.5	1506.9	–25.7	6.9	2.1	1.6
13	1141.6	–19.7	6.3	2.9	2.6	1514.2	–25.5	6.8	2.1	1.6
14	1123.2	–19.0	6.1	3.0	2.7	1520.8	–25.3	6.6	2.2	1.7
15	1104.6	–18.3	5.9	3.1	2.8	1526.8	–25.0	6.4	2.3	1.7
16	1085.9	–17.6	5.6	3.2	2.9	1532.1	–24.7	6.1	2.3	1.8
17	1067.1	–16.9	5.3	3.2	3.0	1536.8	–24.3	5.9	2.4	1.8
18	1048.2	–16.2	5.0	3.3	3.1	1540.8	–24.0	5.6	2.4	1.9
19	1029.3	–15.4	4.7	3.4	3.2	1544.1	–23.6	5.3	2.5	1.9
20	1010.3	–14.7	4.4	3.5	3.2	1546.8	–23.2	5.0	2.5	2.0
21	991.2	–13.9	4.0	3.5	3.3	1548.8	–22.8	4.7	2.5	2.0
22	972.2	–13.2	3.6	3.5	3.3	1550.1	–22.4	4.4	2.5	2.0
23	953.1	–12.5	3.3	3.6	3.4					
24	934.0	–11.7	2.9	3.6	3.4					
25	915.0	–11.0	2.5	3.6	3.4					
26	896.0	–10.3	2.0	3.6	3.4					
27	877.0	–9.6	1.6	3.5	3.4					
28	858.1	–8.9	1.2	3.5	3.3					

and the deviations of the computed transition frequencies from the observed ones as obtained with the CCSD-[4R] method and the three basis sets considered, namely the cc-pVXZ bases with X = D, T, and Q. The deviations obtained with the largest cc-pVQZ basis and including the adiabatic corrections[50] are listed in the column labeled by Q_+.

We observe a systematic improvement of the agreement between the observed and computed frequencies as the basis set is increased. The discrepancies also vary smoothly as we progress towards larger and larger rotational quantum numbers in each branch. For the largest cc-pVQZ basis set considered, these discrepancies stay within 2 to 4 cm^{-1} for all $\Delta v = 1$ bands and only for the *P* branch of the (2,0) overtone band they range up to ≈6 cm^{-1}. These discrepancies are slightly improved (always by less than 1 cm^{-1}) when the adiabatic corrections are added. Clearly, the computed spectra provide an excellent representation of the experimental ones, with an almost constant and very small systematic shift of at most 0.04% in the transition frequencies.

TABLE V

The deviations of the computed transition frequencies from the experimentally (exp) observed ones[52] for the *P* and *R* lines of the (5,4) vibrational band of LiH, as obtained with the CCSD-[4R] method and the cc-pVXZ (X = D, T, and Q) basis sets. The subscript "+" indicates that the adiabatic corrections[50] were added to the potential. All values are in cm^{-1}

J	*P* branch					*R* branch				
	exp	D	T	Q	Q_+	exp	D	T	Q	Q_+
3	1144.9	–20.1	3.6	1.2	0.9					
4	1130.6	–19.9	3.6	1.2	0.9	1244.9	–21.3	3.7	1.2	0.8
5						1255.4	–21.4	3.8	1.3	0.9
6	1101.2	–19.6	3.6	1.3	1.0					
7	1086.1	–19.3	3.6	1.4	1.1	1274.8	–21.6	3.9	1.4	0.9
8	1070.7	–19.1	3.7	1.4	1.1	1283.8	–21.7	4.0	1.4	1.0
9	1055.1	–18.9	3.7	1.5	1.2					
10	1039.2	–18.7	3.8	1.6	1.3					
11	1023.1	–18.5	3.8	1.7	1.4					
12	1006.9	–18.2	3.9	1.8	1.5					
13	990.4	–18.0	3.9	1.9	1.6					
14	973.9	–17.7	4.0	2.0	1.7					
15	957.1	–17.5	4.1	2.1	1.8					

TABLE VI

The deviations of the computed transition frequencies from the experimentally (exp) observed ones[52] for the *P* and *R* lines of the (2,0) vibrational band of LiH, as obtained with the CCSD-[4R] method and the cc-pVXZ (X = D, T, and Q) basis sets. The subscript "+" indicates that the adiabatic corrections[50] were added to the potential. All values are in cm^{-1}

J	*P* branch					*R* branch				
	exp	D	T	Q	Q_+	exp	D	T	Q	Q_+
1	2659.8	–49.1	12.2	2.5	1.6	2701.6	–49.7	12.2	2.4	1.6
2	2644.1	–48.8	12.1	2.5	1.7	2713.9	–49.7	12.2	2.4	1.6
3	2627.7	–48.4	12.1	2.6	1.8	2725.2	–49.7	12.1	2.4	1.6
4	2610.5	–47.9	12.0	2.7	1.9	2735.6	–49.7	12.1	2.5	1.6
5	2592.5	–47.4	11.9	2.8	2.0	2745.1	–49.5	12.0	2.5	1.7
6	2573.8	–46.8	11.8	2.9	2.1	2753.6	–49.3	11.9	2.6	1.7
7	2554.4	–46.2	11.6	3.0	2.3	2761.2	–49.1	11.7	2.7	1.8
8	2534.3	–45.5	11.4	3.2	2.4	2767.8	–48.7	11.6	2.8	1.9
9	2513.5	–44.7	11.2	3.3	2.6	2773.4	–48.3	11.4	2.9	2.0
10	2492.1	–43.9	11.0	3.5	2.7	2778.0	–47.9	11.2	3.0	2.1
11	2470.1	–43.0	10.8	3.6	2.9	2781.6	–47.4	11.0	3.1	2.2
12	2447.5	–42.1	10.5	3.8	3.1	2784.2	–46.9	10.8	3.3	2.4
13	2424.3	–41.2	10.3	4.0	3.3	2785.8	–46.3	10.5	3.4	2.5
14	2400.6	–40.1	9.9	4.1	3.5					
15	2376.3	–39.1	9.6	4.3	3.7					
16	2351.6	–38.0	9.2	4.5	3.9					
17	2326.3	–36.9	8.8	4.7	4.0					
18	2300.6	–35.8	8.4	4.8	4.2					
19	2274.5	–34.6	8.0	5.0	4.4					
20	2248.0	–33.5	7.5	5.1	4.5					
21	2221.1	–32.3	7.1	5.3	4.7					
22	2193.8	–31.1	6.6	5.4	4.8					
23	2166.2	–29.9	6.1	5.5	5.0					
24	2138.2	–28.8	5.6	5.6	5.1					
25	2109.9	–27.6	5.1	5.7	5.2					

Core-Correction Effects

Since in many calculations one decreases the number of explicitly correlated electrons by freezing the core, we wish to examine this effect in the LiH case, where the core electrons represent one-half of the total electron number. For comparison, we also consider the largest first-row hydride, *i.e.*, the HF molecule. Clearly, we can expect the effect of the frozen-core approximation to be the largest for the small LiH species, where the core represents a substantial part of the entire electronic structure.

We thus present in Table VII the differences between the computed and experimental vibrational term values for the ^{7}LiH molecule obtained with all the electrons correlated, and with only the valence electrons correlated. We observe that the core-correlation effects are quite significant, even though not overwhelmingly so considering that in this case half of the electrons are excluded by freezing the core. These effects steadily increase as we proceed to higher and higher vibrational levels, amounting to ≈8 cm^{-1} for the lowest $v = 0$ level and reaching 152 cm^{-1} for the top $v = 22$ level. On the relative scale, however, the effect is largest at the $v = 0$ level, being twice

TABLE VII
The deviation of the FCI/cc-pVTZ vibrational term values from the experimental ones for ^{7}LiH when correlating all the electrons (all) and only the valence electrons (valence), as well as their difference δ representing the core-correlation effects. All values are in cm^{-1}

v	All	Valence	δ	v	All	Valence	δ
0	4.0	–3.8	7.8	12	63.2	–29.3	92.5
1	11.7	–9.7	21.4	13	66.2	–31.8	98.0
2	16.0	–15.4	31.5	14	66.4	–37.0	103.4
3	18.9	–20.4	39.3	15	62.8	–45.9	108.7
4	21.7	–24.4	46.0	16	53.9	–60.0	113.9
5	25.0	–27.2	52.1	17	38.1	–81.0	119.0
6	29.1	–28.9	58.0	18	13.2	–111.0	124.2
7	34.1	–29.7	63.8	19	–23.1	–152.7	129.6
8	39.9	–29.7	69.6	20	–73.8	–209.3	135.5
9	46.2	–29.2	75.4	21	–141.9	–284.3	142.4
10	52.5	–28.6	81.1	22	–230.1	–381.6	151.6
11	58.4	–28.4	86.8				

as large as the discrepancy between the computed and observed term values, while for the highest-lying level (v = 22), this effect represents about two-thirds of the discrepancy between the theory and experiment (even though, for v = 21 level, both effects are of the same size).

For the sake of comparison we present an analogous information for the HF molecule in Tables VIII and IX. In this case we are unable to generate the FCI results at the cc-pVTZ level. We thus present in Table VIII the vibrational energy levels as obtained with the CCSD and CCSD-[4R] methods

TABLE VIII
Vibrational term values for the HF molecule obtained with the CCSD and CCSD-[4R] methods and cc-pVTZ basis set when correlating all the electrons (all) and only the valence electrons (valence), as well as their difference δ representing the core-correlation effects. All values are in cm^{-1}

v	CCSD			CCSD-[4R]		
	All	Valence	δ	All	Valence	δ
0	0.0	0.0	0.0	0.0	0.0	0.0
1	4045.6	4037.8	7.8	4007.5	3999.7	7.8
2	7922.0	7906.4	15.6	7840.0	7824.4	15.6
3	11632.4	11609.2	23.2	11500.4	11477.1	23.3
4	15180.6	15150.1	30.5	14992.0	14961.6	30.4
5	18570.1	18532.6	37.5	18317.8	18280.7	37.1
6	21804.1	21759.9	44.2	21480.5	21437.1	43.4
7	24885.5	24835.0	50.5	24481.4	24432.3	49.1
8	27816.4	27759.6	56.8	27321.0	27266.3	54.7
9	30598.1	30535.0	63.1	29998.0	29938.1	59.9
10	33230.8	33161.4	69.4	32509.8	32444.7	65.1
11	35714.1	35638.1	76.0	34851.5	34781.3	70.2
12	38046.4	37963.5	82.9	37016.5	36941.1	75.4
13	40225.2	40134.8	90.4	38995.2	38914.3	80.9
14	42247.0	42148.5	98.5	40775.1	40688.3	86.8
15	44107.4	43999.8	107.6	42340.1	42246.9	93.2
16	45800.6	45682.8	117.8	43668.5	43568.1	100.4
17	47319.7	47190.1	129.6	44731.6	44623.0	108.6

when all electrons are correlated and when only valence electrons are correlated (note that all the results given in ref.[43] were obtained with frozen core of the fluorine atom). We see that the differences δ, indicating the effect of core electron freezing, are slightly larger for the standard CCSD approach (although, there is practically no difference up to about v = 7 level), and on the absolute scale they are on the same level as for the LiH molecule. However, on the relative scale they are considerably smaller, since the top-level vibrational energy for LiH (20 169.8 cm^{-1} for v = 22) is less than one half of that for the v = 19 level of HF (49 026.5 cm^{-1}).

TABLE IX
Experimental (exp) and theoretical vibrational transition energies $G_{v+1}-G_v$ for the HF molecule as obtained with the CCSD and CCSD-[4R] methods and cc-pVTZ basis set when correlating all the electrons (all) and only the valence electrons (valence), as well as their difference δ representing the core-correlation effects. All values are in cm^{-1}

v	exp[a]	CCSD			CCSD-[4R]		
		All	Valence	δ	All	Valence	δ
0	3961.4	4045.6	4037.8	7.8	4007.5	3999.7	7.8
1	3789.4	3876.4	3868.6	7.8	3832.5	3824.7	7.8
2	3622.0	3710.4	3702.8	7.6	3660.4	3652.7	7.7
3	3458.8	3548.2	3540.9	7.3	3491.6	3484.5	7.1
4	3299.4	3389.5	3382.5	7.0	3325.8	3319.1	6.7
5	3142.8	3234.0	3227.3	6.7	3162.7	3156.4	6.3
6	2988.5	3081.4	3075.1	6.3	3000.9	2995.2	5.7
7	2835.8	2930.9	2924.6	6.3	2839.6	2834.0	5.6
8	2683.5	2781.7	2775.4	6.3	2677.0	2671.8	5.2
9	2530.5	2632.7	2626.4	6.3	2511.8	2506.6	5.2
10	2375.5	2483.3	2476.7	6.6	2341.7	2336.6	5.1
11	2216.5	2332.3	2325.4	6.9	2165.0	2159.8	5.2
12	2051.7	2178.8	2171.3	7.5	1978.7	1973.2	5.5
13	1877.8	2021.8	2013.7	8.1	1779.9	1774.0	5.9
14	1691.7	1860.4	1851.3	9.1	1565.0	1558.6	6.4
15	1488.1	1693.2	1683.0	10.2	1328.4	1321.2	7.2
16	1261.5	1519.1	1507.3	11.8	1063.1	1054.9	8.2

[a] From ref.[56]

Of course, this effect is much smaller when we consider the experimentally observed transition frequencies, as shown in Table IX. Indeed, the largest difference δ between the transition energies obtained with all the electrons and with only the valence electrons correlated amounts to about ≈10 cm^{-1} at the cc-pVTZ level. This difference is again slightly smaller (by ≈4 cm^{-1}) for the highest considered level when the CCSD-[4R] method is used rather than the standard CCSD.

CONCLUSIONS

On the basis of the above presented illustrative examples, as well as from the more comprehensive results given earlier[32–44], we can conclude that the ecCCSD approaches are capable of significantly extending the range of applicability of the standard CCSD method once the quasidegeneracy effects become more significant and the nondynamic correlation plays a non-negligible role or, in fact, a rather essential role as in the case of the N_2 molecule[37,40]. Both the RMR CCSD and CCSD-[*M*R] methods that employ a modest size MR CISD wave function as the external source of information concerning the higher-than-pair clusters, are capable of yielding very accurate potentials over the entire range of geometries and thus highly accurate ro-vibrational spectra.

Remarkably enough, both the RMR CCSD and CCSD-[*M*R] methods yield very similar results in spite of their entirely different design and structure, as long as we employ the same external-source wave function. This clearly indicates that the nondynamic correlation effects can be accounted for either by appropriately correcting the one- and two-body amplitudes *via* RMR CCSD or by projecting onto the MR CISD wave function when computing the energy *via* the CCSD-[*M*R] method.

Our results also reaffirm the importance of the basis set size when we wish to achieve a good agreement with experiment. In the case of a small four-electron system like LiH, when we are able to generate the FCI energies even with a relatively good basis set, such as the cc-pVTZ basis, we clearly see that the discrepancies with experiment arise almost entirely due to the basis set limitation, rather than due to the approximations that are inherent in the ecCCSD methods employed.

Our results leave little doubt that either of the ecCCSD methods employing the MR CISD wave function as the source of nondynamic correlation effects is capable of producing highly accurate and reliable potentials and the implied spectroscopic data.

The continued support by the National Science and Engineering Research Council of Canada (J. Paldus) is gratefully acknowledged. We are also obliged to Prof. R. J. LeRoy for letting us use his LEVEL 6.1 codes and for his valuable comments, as well as to Prof. P. F. Bernath for his expert advice concerning the sources of the experimental data and their reliability.

REFERENCES

1. Picard É.: *Jubilé Scientifique de M. Élie Cartan célébré à la Sorbonne le 18. Mai 1939*, p. 8. Gauthiers–Villars, Paris 1939.
2. a) Hartree D. R.: *Proc. Cambridge Philos. Soc.* **1928**, *24*, 89; b) Hartree D. R.: *Proc. Cambridge Philos. Soc.* **1928**, *24*, 111; c) Hartree D. R.: *Proc. Cambridge Philos. Soc.* **1928**, *24*, 426.
3. Fock V.: *Z. Phys.* **1930**, *61*, 126.
4. Roothaan C. C. J.: *Rev. Mod. Phys.* **1951**, *23*, 69.
5. Wahl A. C.: *J. Chem. Phys.* **1964**, 41, 2600.
6. Shelton D. P., Rice J. E.: *Chem. Rev. (Washington, D. C.)* **1994**, *94*, 3.
7. Piecuch P., Kondo A. E., Špirko V., Paldus J.: *J. Chem. Phys.* **1996**, *104*, 4699.
8. Wilson S.: *Electron Correlation in Molecules*. Clarendon, Oxford 1984.
9. Harris F. E., Monkhorst H. J., Freeman D. L.: *Algebraic and Diagrammatic Methods in Many-Fermion Theory*. Oxford University Press, Oxford 1992.
10. Paldus J. in: *Atomic, Molecular, and Optical Physics Handbook* (G. W. F. Drake, Ed.), Chap. 5. AIP Press, Woodbury (NY) 1996.
11. Čížek J.: *J. Chem. Phys.* **1966**, *45*, 4256.
12. Čížek J.: *Adv. Chem. Phys.* **1969**, *14*, 35.
13. Bartlett R. J. in: *Modern Electronic Structure Theory,* Part II (D. R. Yarkony, Ed.), Vol. 2, p. 1047. World Scientific, Singapore 1995.
14. Paldus J., Li X.: *Adv. Chem. Phys.* **1999**, *110*, 1.
15. Raghavachari K.: *J. Chem. Phys.* **1985**, *82*, 4607.
16. Urban M., Noga J., Cole S. J., Bartlett R. J.: *J. Chem. Phys.* **1985**, *83*, 4041.
17. a) Paldus J. in: *Methods in Computational Molecular Physics; NATO Advanced Study Institute, Series B: Physics* (S. Wilson and G. H. F. Diercksen, Eds), Vol. 293, p. 99. Plenum Press, New York 1992; b) Paldus J. in: *Relativistic and Electron Correlation Effects in Molecules and Solids; NATO Advanced Study Institute, Series B: Physics* (G. L. Malli, Ed.), Vol. 318, p. 207. Plenum Press, New York 1994.
18. a) Mášik J., Hubač I., Mach P.: *J. Chem. Phys.* **1998**, *108*, 6571; b) Pittner J., Nachtigall P., Čársky P., Mášik J., Hubač I.: *J. Chem. Phys.* **1999**, *110*, 10275.
19. Mahapatra U. S., Datta B., Mukherjee D.: *J. Chem. Phys.* **1999**, *110*, 6171.
20. a) Meller J., Malrieu J.-P., Caballol R.: *J. Chem. Phys.* **1996**, *104*, 4068; b) Peris G., Planelles J., Malrieu J.-P., Paldus J.: *J. Chem. Phys.* **1999**, *110*, 11708.
21. a) Meissner H., Paldus J.: *J. Chem. Phys.* **2000**, *113*, 2594; b) Meissner H., Paldus J.: *J. Chem. Phys.* **2000**, *113*, 2612; c) Meissner H., Paldus J.: *J. Chem. Phys.* **2000**, *113*, 2622; d) Meissner H., Paldus J.: *Int. J. Quantum Chem.* **2000**, *80*, 782; e) Meissner H., Ema I.: *J. Mol. Struct. (THEOCHEM)* **2001**, *547*, 171.
22. Paldus J., Čížek J., Shavitt I.: *Phys. Rev. A: At., Mol., Opt. Phys.* **1972**, *5*, 50.
23. a) Čížek J., Paldus J.: *Int. J. Quantum Chem.* **1971**, *5*, 359; b) Paldus J., Čížek J., Jeziorski B.: *J. Chem. Phys.* **1989**, *90*, 4356.

24. Paldus J. in: *Self-Consistent Field: Theory and Applications* (R. Carbó and M. Klobukowski, Eds), p. 1. Elsevier, Amsterdam 1990.
25. a) Paldus J., Čížek J., Takahashi M.: *Phys. Rev. A: At., Mol., Opt. Phys.* **1984**, *30*, 2193; b) Paldus J., Takahashi M., Cho R. W. H.: *Phys. Rev. B: Condens. Matter* **1984**, *30*, 4267.
26. Piecuch P., Toboła R., Paldus J.: *Phys. Rev. A: At., Mol., Opt. Phys.* **1996**, *54*, 1210.
27. a) Paldus J., Planelles J.: *Theor. Chim. Acta* **1994**, *89*, 13; b) Planelles J., Paldus J., Li X.: *Theor. Chim. Acta* **1994**, *89*, 33; c) Planelles J., Paldus J., Li X.: *Theor. Chim. Acta* **1994**, *89*, 59.
28. Peris G., Planelles J., Paldus J.: *Int. J. Quantum Chem.* **1997**, *62*, 137.
29. a) Li X., Peris G., Planelles J., Rajadell F., Paldus J.: *J. Chem. Phys.* **1997**, *107*, 90; b) Peris G., Rajadell F., Li X., Planelles J., Paldus J.: *Mol. Phys.* **1998**, *94*, 235.
30. Stolarczyk L. Z.: *Chem. Phys. Lett.* **1994**, *217*, 1.
31. a) Li X., Paldus J.: *J. Chem. Phys.* **1994**, *101*, 8812; b) Jeziorski B., Paldus J., Jankowski P.: *Int. J. Quantum Chem.* **1995**, *56*, 129.
32. Li X., Paldus J.: *J. Chem. Phys.* **1997**, *107*, 6257.
33. a) Li X., Paldus J.: *J. Chem. Phys.* **1998**, *108*, 637; b) Li X., Paldus J.: *J. Chem. Phys.* **1999**, *110*, 2844.
34. a) Li X., Paldus J.: *Collect. Czech. Chem. Commun.* **1998**, *63*, 1381; b) Li X., Paldus J.: *Chem. Phys. Lett.* **1998**, *286*, 145.
35. a) Li X., Grabowski I., Jankowski K., Paldus J.: *Adv. Quantum Chem.* **1999**, *36*, 231; b) Peris G., Planelles J., Malrieu J.-P., Paldus J.: *J. Chem. Phys.* **1999**, *110*, 11708; c) Planelles J., Peris G., Paldus J.: *Int. J. Quantum Chem.* **2000**, *77*, 693.
36. a) Li X., Paldus J.: *Mol. Phys.* **2000**, *98*, 1185; b) Li X., Paldus J.: *Int. J. Quantum Chem.* **2000**, *80*, 743.
37. Li X., Paldus J.: *J. Chem. Phys.* **2000**, *113*, 9966.
38. Paldus J., Li X.: *Top. Curr. Chem.* **1999**, *203*, 1.
39. Li X.: *J. Mol. Struct. (THEOCHEM)* **2001**, *547*, 69.
40. a) Li X., Paldus J.: *J. Chem. Phys.* **2001**, *115*, 5759; b) Li X., Paldus J.: *J. Chem. Phys.* **2001**, *115*, 5774.
41. Paldus J., Li, X. in: *Advances in Quantum Many-Body Theory* (R. F. Bishop, T. Brandes, K. A. Gernoth, N. R. Walet and Y. Xian, Eds), Vol. 5, p. 393. World Scientific, Singapore 2002.
42. Li X., Paldus J. in: *Low-Lying Potential–Energy Surfaces* (M. R. Hoffmann and K. G. Dyall, Eds), ACS Symposium Series No. 828, p. 10. ACS Books, Washington 2002.
43. Li X., Paldus J.: *J. Chem. Phys.* **2002**, *117*, 1941.
44. Li X., Paldus J.: *J. Chem. Phys.* **2003**, *118*, 2470.
45. Piecuch P., Kowalski K. in: *Computational Chemistry: Reviews of Current Trends* (J. Leszczynski, Ed.), Vol. 5, p. 1. World Scientific, Singapore 2000.
46. a) Kowalski K., Piecuch P.: *J. Chem. Phys.* **2000**, *113*, 18; b) Kowalski K., Piecuch P.: *J. Chem. Phys.* **2000**, *113*, 5644; c) Kowalski K., Piecuch P.: *J. Mol. Struct. (THEOCHEM)* **2001**, *547*, 191.
47. Jankowski K., Paldus J., Piecuch P.: *Theor. Chim. Acta* **1991**, *80*, 223.
48. a) Kowalski K., Piecuch P.: *Chem. Phys. Lett.* **2001**, *344*, 165; b) Piecuch P., Kucharski S. A., Kowalski K.: *Chem. Phys. Lett.* **2001**, *344*, 176; c) Piecuch P., Kucharski S. A., Špirko V., Kowalski K.: *J. Chem. Phys.* **2001**, *115*, 5796.
49. Kutzelnigg W.: *Mol. Phys.* **1998**, *94*, 65.
50. Chan Y. C., Harding D. R., Stwalley W. C., Vidal C. R.: *J. Chem. Phys.* **1986**, *85*, 2436.
51. Stwalley W. C., Zemke W. T.: *J. Phys. Chem. Ref. Data* **1993**, *22*, 87.

52. Dulick M., Zhang K. Q., Guo B., Bernath P. F.: *J. Mol. Spectrosc.* **1998**, *188*, 14.
53. Mann D. E., Thrush B. A., Lide D. R., Jr., Ball J. J., Acquista N.: *J. Chem. Phys.* **1961**, *34*, 420.
54. Webb D. U., Rao K. N.: *J. Mol. Spectrosc.* **1968**, *28*, 121.
55. Di Leonardo G., Douglas A. E.: *Can. J. Phys.* **1973**, *51*, 434.
56. a) Coxon J. A., Hajigeorgiou P. G.: *J. Mol. Spectrosc.* **1989**, *133*, 45; b) Coxon J. A., Hajigeorgiou P. G.: *J. Mol. Spectrosc.* **1990**, *142*, 254.
57. Dunning T. H., Jr.: *J. Chem. Phys.* **1989**, *90*, 1007.
58. Basis sets were obtained from the *Extensible Computational Chemistry Environment Basis Set Database*, as developed and distributed by the Molecular Science Computing Facility, Environmental and Molecular Sciences Laboratory, which is part of the Pacific Northwest Laboratory, P.O. Box 999, Richland, WA 99352, U.S.A., and funded by the U.S. Department of Energy. The Pacific Northwest Laboratory is a multi-program laboratory operated by Battelle Memorial Institute for the U.S. Department of Energy under the contract DE-AC06-76RLO 1830. Contact David Feller or Karen Schuchardt for further information.
59. The GAMESS system of programs by M. Dupuis, D. Spangler, and J. J. Wendoloski, National Resource for Computations in Chemistry, Software Catalog (University of California, Berkeley (CA) 1980), *Program QG01*; Schmidt M. W., Baldridge K. K., Boatz J. A., Elbert S. T., Gordon M. S., Jensen J. H., Koseki S., Matsunaga M., Nguyen K. A., Su S. J., Windus T. L., Dupuis M., Montgomery J. A.: *J. Comput. Chem.* **1993**, *14*, 1347.
60. LeRoy R. J.: *LEVEL 7.4, A Computer Program Solving the Radial Schrödinger Equation for Bound and Quasibound Levels, and Calculating Various Expectation Values and Matrix Elements*. Chemical Physics Research Report CP-642R, University of Waterloo 2001.
61. Kosman W. M., Hinze J.: *J. Mol. Spectrosc.* **1975**, *56*, 93.
62. Vidal C. R., Scheingraber H.: *J. Mol. Spectrosc.* **1977**, *65*, 46.
63. a) Coxon J. A.: *J. Mol. Spectrosc.* **1986**, *117*, 361; b) Coxon J. A.: *J. Mol. Spectrosc.* **1989**, *133*, 96.
64. a) Peterson K. A., Dunning T. H., Jr.: *J. Chem. Phys.* **1995**, *102*, 2032; b) Peterson K. A., Dunning T. H., Jr.: *J. Chem. Phys.* **1995**, *103*, 4572.